Image-based catheter tip tracking during cardiac ablation therapy

Marcel Schenderlein[1]
marcel.schenderlein@uni-ulm.de
Volker Rasche[2]
volker.rasche@uniklinik-ulm.de
Klaus Dietmayer[1]
klaus.dietmayer@uni-ulm.de

[1] Institute of Measurement, Control, and Microtechnology
Ulm University, Ulm, Germany

[2] Department of Internal Medicine II
University Hospital of Ulm,
Ulm, Germany

Abstract

Image-based catheter tip tracking has the potential to support electro-physiological interventions by additional information such as the three-dimensional position and orientation of the catheters. However, curve deformation algorithms commonly used to reconstruct elongated objects from biplane X-ray fluoroscopy images do not guarantee a correct detection of the tip position. The proposed approach combines a curve deformation algorithm and a biplane template matching technique which is based on virtual reconstructions of the catheter tip projection. It allows for an accurate and robust three-dimensional tracking of the catheter tip and orientation with a mean position error of 0.80 ± 0.61 mm and a mean tip distance of 0.72 ± 0.52 mm for 94 % of all frames. This is demonstrated on patient data sets by a comparison to previously published approaches.

1 Introduction

In electro-physiological (EP) interventions several catheters are navigated inside the heart chambers. The main purpose of this procedure is to locate sources of arrhythmia and successively destroy the involved tissue. Therefore an ablation catheter is led to these positions under guidance of X-ray fluoroscopy images. The knowledge of the three-dimensional (3D) position and orientation of the ablation catheter tip is of immense importance to the physician. It must be ensured that ablation sites are created without gaps by placing concatenated lesions or by pulling the catheter along involved structures without interruption. However, in standard EP interventions, the positions of the catheters are only inferred from their projections onto the X-ray fluoroscopy images. For support, biplane X-ray systems provide a stereoscopic setting. Still, mentally reconstructing the 3D catheters, as it is common practice for physicians, remains a difficult task. Image-based reconstruction from the standard X-ray fluoroscopy images, present in every intervention, has the potential to support the physician with additional information such as 3D position and orientation of the catheters. Catheter tip tracking may also be used in combination with cardiac augmented reality systems like the work presented by Ector *et al*. [3].

Image-based 3D tracking of the catheter tip or its whole body represents a continuous reconstruction from the two-dimensional (2D) biplane images. Recent work in this field has

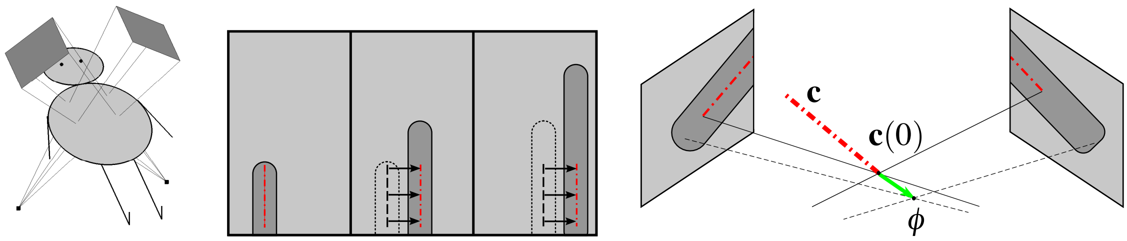

(a) (b) (c)

Figure 1: (a) The stereoscopic biplane X-ray image acquisition geometry. The image intensifier planes are depicted in dark gray and the X-ray sources as black squares. (b) Result of a missing explicit tip tracking. The catheter (dotted: previous, dark gray: current) moves to the upper right corner in these three consecutive image frames. The curve (dashed: previous, dash-dotted: current) is deformed in order to align with the catheter centerline but the tip position is not taken into account. (c) Idealized geometry with curve $\mathbf{c}$ and its projections onto the images (dash-dotted red lines). The 2D catheter tips are reconstructed to the point ϕ. The green arrow depicts the deformation force created by the distance of the curve tip $\mathbf{c}(0)$ to ϕ.

been published on 3D tracking of vascular structures [2], guide-wires [1] and EP catheters [5]. In [2] the tip of a vessel is tracked implicitly by tracking the whole vessel shape based on curve optimization methods. However, optimal curves may also be found at positions, where it is not guaranteed, that one of their end points is located exactly at the catheter tip. A separate tip detection stage, composed of finding the most likely tip position by finding the intensity edge along the curve and a short extrapolated path, was used in [1] and [5]. This approach, however, is handicapped in the presence of high foreshortening, background clutter and converged curves not pointing exactly in the direction of the catheter tip.

In order to overcome these limitations, we propose a biplane template matching technique based on virtual reconstructions of the catheter tip projection. Our goal is to enhance the accuracy of the tip localization and the tracking rate for the aforementioned applications.

2 Methods

In our two-stage approach, the catheter tip is tracked in 3D space by reconstructing the front centerline of the catheter from biplane X-ray fluoroscopy images using a curve deformation algorithm. After its convergence, in the second stage, the catheter tip position is estimated by biplane template matching and an enhanced curve deformation.

2.1 Data acquisition

The image data is acquired on a Philips Integris BH5000 biplane X-ray image intensifier system (Philips Medical Systems, Best, Netherlands) which consists of two X-ray sources and image intensifiers (see 1(a)). It provides two image sequences at 12.5 fps showing the volume of interest from right anterior oblique (RAO) 30° and left anterior oblique (LAO) 40°. The systems geometry was calibrated using a calibration phantom before the intervention.

As in our previous work [5] the image sequences are acquired in interlaced mode. However, in the following explanation synchronous sequences are assumed for brevity.

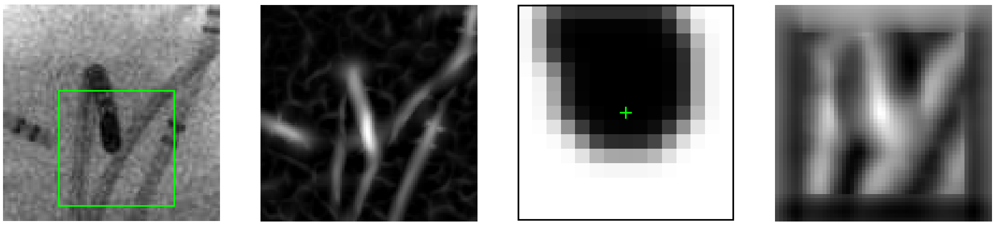

(a) (b) (c) (d)

Figure 2: (a) Part of the original X-ray image with template search window (green rectangle). (b) Corresponding result of the line-enhancing filter. (c) Generated tip template. Note, that because of perspective foreshortening, the catheter tip (green cross) is not located at the object edge. (d) Corresponding 2D correlation result for the template search window with white color indicating high correlation.

2.2 Curve deformation

The first stage for the catheter tip tracking is the 3D reconstruction of the frontal part of the catheter path. For this purpose we find the optimal 3D curve $\mathbf{c}(s) = (x(s), y(s), z(s))$, with s being the normalized arc length, which minimizes the energy functional

$$E(\mathbf{c}(s)) = \int_s (E_{int}(\mathbf{c}(s)) + E_{image}(\mathbf{c}(s)) + E_{curv}(\mathbf{c}(s)))\, ds, \qquad (1)$$

where $E_{int} = \beta \cdot |\mathbf{c}_{ss}(s)|^2$ is the internal energy, which restricts the curvature and E_{image} depicts the image energy, which guides the deformation towards the image features (details below). $E_{curv} = \omega \cdot ||\mathbf{c}_s(s)|^2 - d^2|^2$ represents the curvilinear reparametrization energy [4], which keeps the sampling points along the curve at equal distance d and thus keeps a constant total length of the curve. The parameters β and ω describe the influence of the single energies on the total energy. The image energy E_{image} for the 3D curve is a linear combination of the 2D image energies extracted at each curve projection in both of the images. The image feature is the result of a line-enhancing filter based on eigenvalue evaluation of each pixels Hessian (see fig. 2(a) and 2(b)).

As a result of this stage, the 3D curve is deformed in a way that its projections onto the two views match with the catheter path. However, an optimal curve position may be found everywhere along the catheter path. It is not guaranteed that the curve tip projections align with the catheter tips in the images (see fig. 1(b)). This is most prominent if the catheter was moved along its tangential direction between two image frames. In order to counteract this effect, a second stage performs an explicit catheter tip detection.

2.3 Catheter tip detection

We assume, that when the curve deformation has converged, the curve tip is positioned in the vicinity of the true catheter tip and the orientation of the curve is close to the true catheter orientation. Meeting these requirements, we are able to produce expected projections of the catheter tip onto the image planes by a catheter model ray-casting method (see fig. 2(c)). These virtual tip templates are then matched with a search window of their respective X-ray fluoroscopy images by normalized 2D cross-correlation (see fig. 2(d)). From the two 2D positions of the maximum peaks of each correlation in the image planes, an estimated 3D tip position ϕ is reconstructed (see fig. 1(c)). The distance between ϕ and the curve tip position leads to an external constraint energy [4] with weighting parameter ψ:

$$E_c = \psi \cdot |\phi - \mathbf{c}(0)|^2. \quad (2)$$

Subsequently, the curve deformation algorithm is run again until convergence, but now including E_c added to the sum of energies. This acts like a spring on the tip of the curve at $s = 0$ and pulls it towards the correct catheter tip.

2.4 Catheter tip tracking

When the two stages have converged, the curve is saved at the current time step and a new image pair is acquired. Again, the two outlined stages are carried out until convergence. By looping this process, the algorithm continuously reconstructs and tracks the catheter tip.

3 Results

We evaluate the accuracy of our algorithm during the tracking of the front part of the ablation catheter (fig. 2(a)). The curve ranges from the tip to the last electrode at a length of 18 mm. Three sequences of three different patients comprising a total of 588 frames are processed. All sequences include an active motion applied by the physician of either pulling or pushing the catheter additional to the anatomic motion. The methods we compare are: (a) a curve deformation without tip detection as in [2], (b) a curve deformation with tip detection based on edge finding as in [5], and (c) our proposed approach. Further, we compare three variations of our approach: (d) with continuous template update for each iteration, (e) only using stage two, and (f) only using stage two with continuous template update.

Each catheter reconstruction result is compared to a ground truth position, created by a 3D reconstruction of manually labeled 2D positions. The interlaced acquisition of the image sequences was taken into account by reconstructing the points similar to the image force reconstruction in [5]. For evaluation, the mean 3D euclidean distance in normal direction of overlapping curve segments e_{cur} and a separate 3D euclidean tip distance e_{tip} is computed for each curve. Furthermore a rate r is specified, which embodies the amount of frames on which the algorithms did perform well enough. We call r the tracking rate. It is measured as the ratio of reconstructions having e_{cur} and e_{tip} below 4 mm to the total number of reconstructions. This threshold is motivated by a compromise between high accuracy and high tracking rate. Only the reconstructions which meet these requirements are included in the position error evaluations. The results for each sequence are displayed in figure 3 as the mean e_{cur}, the mean e_{tip} and the tracking rate. These results clearly indicate the gain in tip localization accuracy and tracking rate of the proposed approach. The variations (d), (e), and (f) do not improve the overall results. The total mean 3D curve position error over all sequences for the proposed approach is 0.80 ± 0.61 mm with a mean tip distance of 0.72 ± 0.52 mm for 94 % of all frames. Considering all frames the accuracy is $\bar{e}_{cur} = 1.07 \pm 1.41$ mm and $\bar{e}_{tip} = 1.07 \pm 1.96$ mm. The evaluation is performed retrospectively, since the methods are implemented in MATLAB (The MathWorks, Inc.) without real-time considerations.

4 Conclusion

We outlined an approach which addresses the explicit EP catheter tip tracking, which we evaluated on three sequences of the ablation catheter. The results indicate a superior per-

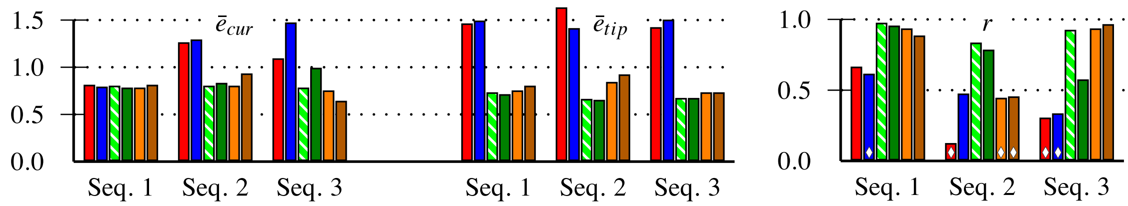

Figure 3: (left) The mean curve position error $\bar{e}_{cur}$ $[mm]$. (middle) The mean tip distance $\bar{e}_{tip}$ $[mm]$. (right) The tracking rate r. The diamond indicates algorithms not recovering from temporary errors in particular sequences. The different methods (see sec. 3) are indicated from the left to the right bar in each bar group as method (a) in red, (b) in blue, the proposed method (c) in hatched green-white, (d) in dark green, (e) in orange and (f) in dark orange.

formance compared to previous approaches. We also compared different variations of our method and the proposed one had the highest overall performance. The evaluations showed that an explicit detection of the catheter tip which accounts for the special shape of the tip is necessary in order to achieve good tracking results with high accuracy. Our approach meets the clinical accuracy requirements and thus it has the potential to be an essential component in an image-based augmented reality system for cardiac ablation therapies to support quick, safe and easy ablation procedures. Nevertheless there are still situations in which the algorithm temporarily fails, so in our future work, we want to further enhance the tracking rate by using this technique at all electrode positions as well as introducing a re-initialization stage. We also plan to implement the algorithm in C++ and if feasible use the GPU in order to run it in a clinical real-time framework.

Acknowledgments

The authors would like to thank Dr. Grossmann and Dr. Stiller of the Department of Internal Medicine II of the University Hospital Ulm, Ulm, Germany, for their assistance in acquiring image data and for biomedical advice.

References

[1] S.A.M. Baert, E.B. van de Kraats, T. van Walsum, M.A. Viergever, and W.J. Niessen. Three-dimensional guide-wire reconstruction from biplane image sequences for integrated display in 3-d vasculature. *IEEE Trans Med Imag*, 22(10):1252–1258, Oct 2003.

[2] C. Canero, P. Radeva, R. Toledo, and J. J. Villanueva. 3d curve reconstruction by biplane snakes. In *Proc. Int. Conf. Pattern Recognition*, pages 563–566. IEEE, 2000.

[3] J. Ector, S. De Buck, W. Huybrechts, D. Nuyens, S. Dymarkowski, J. Bogaert, F. Maes, and H.Heidbüchel. Biplane three-dimensional augmented fluoroscopy as single navigation tool for ablation of atrial fibrillation: Accuracy and clinical value. *Heart Rhythm*, 5(7):957–964, 2008.

[4] M. Jacob, T. Blu, and M. Unser. Efficient energies and algorithms for parametric snakes. *IEEE Trans Imag Proc*, 13(9):1231–1244, Sept. 2004.

[5] M. Schenderlein, S. Stierlin, R. Manzke, V. Rasche, and K. Dietmayer. Catheter tracking in asynchronous biplane fluoroscopy images by 3d b-snakes. In *Proc. SPIE Medical Imaging*, volume 7625, page 762564, 2010.